Orbital: The Electronic Journal of Chemistry
journal homepage: www.orbital.ufms.br
e-ISSN 1984-6428

| Vol 12 | | No. 4 | | October-December 2020 |

FULL PAPER

New Small Compounds Based on Thienylenevinylene with D-A-D Structure for BHJ Applications: Theoretical Study

Aziz El Alamy*[a], Mohamed Bourass[b], Amina Amine[a], Rachid Kcimi[a], and Mohammed Bouachrine[a]

[a] Moulay Ismail University Faculty of Sciences Meknes, Morocco.
[b]Sidi Mohammed bno Abdellah University, Faculty of Sciences Dhar Mahrez, Fez, Morocco.

Article history: Received: 19 July 2020; revised: 07 September 2020; accepted: 06 October 2020. Available online: 28 December 2020. DOI: http://dx.doi.org/10.17807/orbital.v12i4.1524

Abstract:

In this work, ten new small molecules based on Thienylenevinylene as a donor and heterocyclic group A as acceptor of electrons with the donor-acceptor-donor D-A-D structure were studied by density functional theory (DFT) and time-dependent DFT (TDDFT) methods using the Gaussian09 program. The geometric and electronic properties of these compounds have been analyzed and reported by using the DFT /B3LYP level with 6-31G (d,p) basis set. Thus, we calculated the optical properties (absorption/emission) using the TDDFT/CAM-B3LYP/6-31G (d,p) method. The influence of the change of acceptor (π-linker) on the electrochemical, photovoltaic and optic properties has been investigated and discussed. The studied compounds have low energy gap which decreases by going from C1 to C10, this improve the intramolecular charge transfer in these molecules. This work shows that the studied compounds are promising and have good properties for optoelectronic and photovoltaic applications, especially in BHJ solar cells with maximum power conversion efficiency (PCE) of 10% for C7 and C9.

Keywords: thienylenevinylene; DFT; HOMO; LUMO; gap energy; BHJ organic solar cells

1. Introduction

Organic solar cells based on conjugated small molecules are the first organic photovoltaic cells that were made at the end of the 1950s. These materials have several advantages, such as well-defined molecular structures, easier purification and reproducibility. As a result, several research efforts have been devoted to the development of small molecule used in bulk heterojunction (BHJ) cells in recent years, and the conversion efficiency has been progressively improved [1-9].

An interesting approach is to use molecules incorporating an electron acceptor group within the donor conjugate system to improve optoelectronic properties and create good intramolecular charge transfer (ICT).

Small molecules based on Thienylenevinylene show interesting optoelectronic and photovoltaic performances as donor materials in photovoltaic devices [10,11]. Similarly, these compounds of linear structure and symmetrical architecture (D-A-D) have also led to efficient photovoltaic devices in bilayer or bulk heterojunction, with a heterocyclic electron acceptor group inserted as bridge and which has affected the energy levels of the frontier orbitals (decrease in LUMO and increase in HOMO) and consequently the reduction of the bandgap width depending on the nature of this group. This molecular structure improves charge transfer, thus covering a large absorption band in the visible and near-infrared range.

In this work, in order to save costs and synthesis efforts as well as to provide a visual aid to understand how the molecular structure affects their properties, we were interested in the theoretical study of the structural, optoelectronic and photovoltaic properties through the DFT theory of a series of D-A-D systems based on Trithienylenevinylene by incorporating in their

*Corresponding author. E-mail: elalamyaziz@gmail.com

core various heterocyclic acceptor groups (A) as shown in Figure 1. We used the DFT approach with B3LYP exchange-correlation function combined with 6-31G(d,p) basis set to calculate and to examine the structural properties (optimization, bond lengths) and electronic properties (HOMO, LUMO, Voc, α) as well as the electrochemical and charge transport properties (ionization potential (IP), electron density (ED), reorganization energy). While the absorption and emission properties of these compounds were studied using the TD-DFT/CAM-B3LYP/6-31G (d, p) method.

Simulation of these compounds as donor materials in BHJ solar cells combined with the $PC_{60}BM$, $PC_{70}BM$ and $PC_{71}BM$ acceptors, and based on Scharber's model, the estimated conversion efficiency gives best values which can be as high as 10% with some compounds.

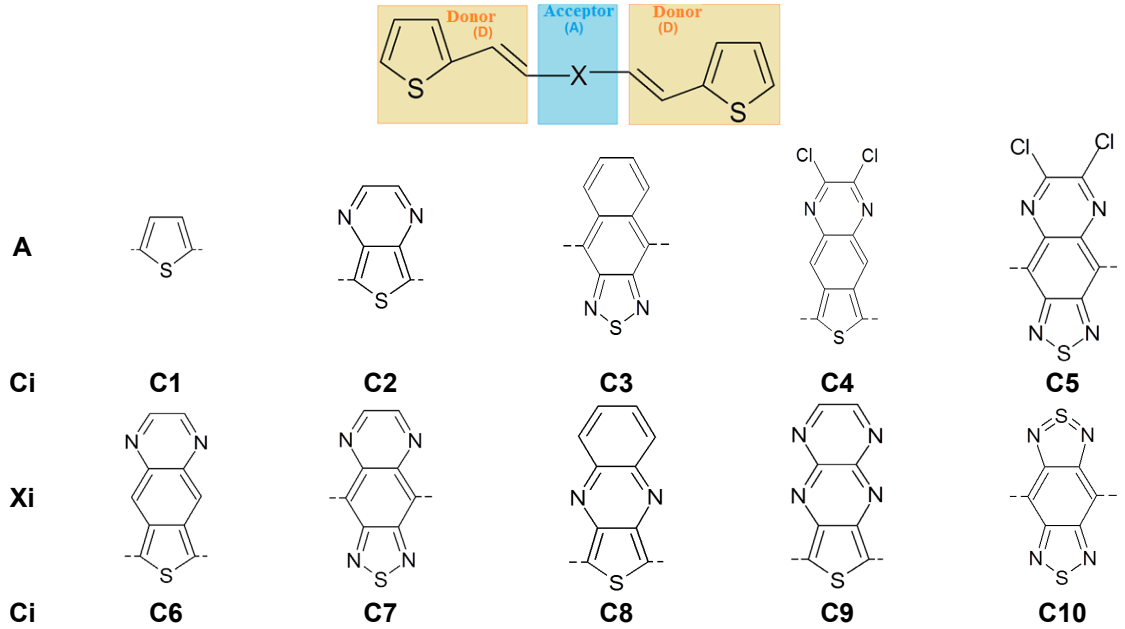

Figure 1. Chemical structures of the studied molecules.

2. Material and Methods

2.1 Calculation methodology

In order to study the relationships between structure and optoelectronic properties, all quantum calculations were performed using Gaussian09 package [12]. The optimization geometry and electronic properties of all molecules in the ground state have been carried and calculated out by the DFT/B3LYP/6-31G(d,p) method [13,14]. Basing on the optimized structures, the absorption spectra and optic properties parameters were calculated by using TD-DFT approach with coulomb-attenuated hybrid exchange-correlation functional (CAM-B3LYP) and 6-31G(d,p) basis set [15]. The choice of the CAM-B3LYP functional is to estimate successfully the transition energies as reported in the literature [16-19]. In addition, the injection and charge transfer properties (ionization potential, electron affinity and reorganization energy) of the studied compounds were analyzed and discussed. Finally, photovoltaic parameters and conversion efficiency estimation were determined in the BHJ structure of an active layer formed by a mixture (Donor/Acceptor) of our compounds as electron donor materials and fullerene derivatives as acceptors.

3. Results and Discussion

3.1 Geometrical and optoelectronic properties

3.1.1 Geometrical structures

The optimized structures of the studied molecules obtained by DFT/B3LYP/ 6-31G(d) method in the ground states are depicted in Figure 2. According to these results, it can be seen that all compounds have similar conformations (planar

conformation). This is attributed to the vinyl groups inserted between the aromatic rings. In addition, we noted a slight reduction in the bond lengths d1 and d2 (between donor and acceptor groups) of the order of 0.01Å relative to C1 (Table 1). This improves the intramolecular charge transfer within these systems.

Table 1. Bond lengths d1 and d2 obtained by B3LYP/6-31G (d, p) method.

Ci	C1	C2	C3	C4	C5	C6	C7	C8	C9	C10
d1(Å)	1.4382	1.4284	1.4270	1.4280	1.4314	1.4273	1.4305	1.4247	1.4248	1.4245
d2(Å)	1.4382	1.4284	1.4270	1.4280	1.4314	1.4273	1.4305	1.4247	1.4248	1.4245

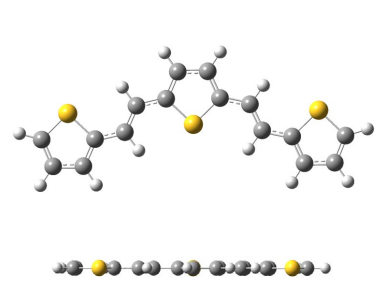

C1

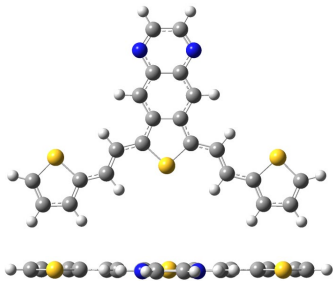

C6

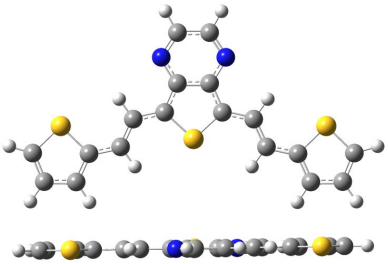

C2

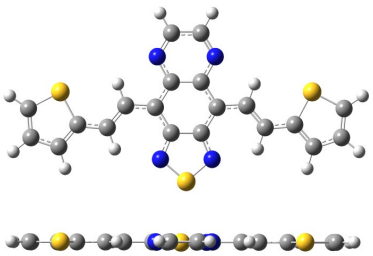

C7

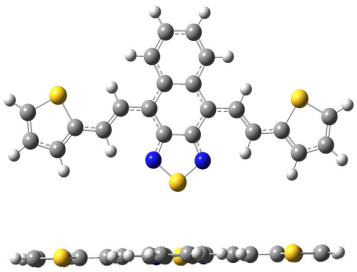

C3

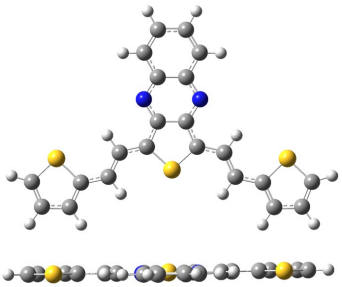

C8

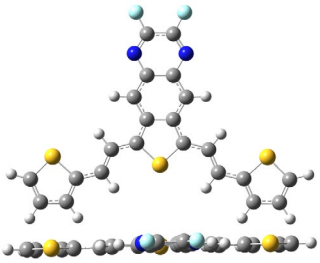

C4

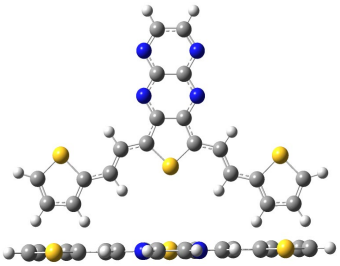

C9

Figure 2. Geometrical structures of the studied molecules optimized by B3LYP/6-31G (d, p) method.

3.1.2 The HOMO, LUMO frontier orbitals and gap energy

The analysis of the highest occupied molecular orbital (HOMO) and lowest unoccupied molecular orbital (LUMO) is very important, because the control of these parameters and even difference between them (gap energy) has become progressively a major topic for the chemical engineering and of functional p-conjugated systems. The calculated values of the HOMO, LUMO and gap energy of all molecules obtained by the by using B3LYP/6-31G (d, p) method are reported in Table 2.

Table 2. Electronic properties of the studied compounds obtained by B3LYP/6-31G(d, p).

Molecule	E_{HOMO} (eV)	E_{LUMO} (eV)	E_g (eV)
C1	-4.89 (-4.95[a])	-2.06 (-2.80[b])	2.83 (2.15[c])
C2	-4.80	-2.69	2.11
C3	-4.76	-2.94	1.82
C4	-4.73	-2.95	1.78
C5	-5.05	-3.29	1.76
C6	-4.59	-2.85	1.73
C7	-4.88	-3.19	1.69
C8	-4.63	-2.98	1.65
C9	-4.82	-3.34	1.48
C10	-4.83	-3.43	1.40

[a]HOMO energy estimated from oxidation onset by cyclic voltammetry (CV); [b]LUMO energy estimated from reduction onset by CV; [c]Electronic bandgap estimated from CV [20].

We found that the HOMO energy of these compounds range from -5.05 to -4.63 eV, while the LUMO range from -3.43 to -2.06 eV. Compared to C1, we noted a stabilization of LUMO energy and destabilization of HOMO, this effect can be explained by the introduction of electron-withdrawing groups as π-linker and the resonance stabilization energy of the aromatic cycles. Therefore, we show that C10 has the lowest LUMO energy (-3.43 eV) compared to other molecules, which can be due to the high electron-withdrawing property of benzobis(thiadiazole) group.

Going from C1 to C10, we noted a remarkable decrease in the gap energy depending on the increase of electron-withdrawing strength of the introduced acceptor fragment. C10 has the lowest gap energy (1.4eV), which is attributed to the introduction of the benzobis (thiadiazole) group which has the highest electron-withdrawing force. Finally, the studied compounds have small energy gaps; this property gives them good candidates for applications in optoelectronic devices, especially in organic solar cells.

The electron density distributions of the frontier orbitals (HOMO and LUMO) on the studied molecules backbone are shown in Figure 3.

We noted that the distribution of electron density in the frontier molecular orbitals is similar for all molecules. As shown in Figure 3, the HOMO of all the compounds is located on the entire system and possesses a π-antibonding character between two adjacent fragments and p bonding character within subunit. Whereas, the LUMO is mainly distributed on the acceptor group (π-lincker) and we show that the LUMO exhibits a π-bonding character within subunit. This means that the electronic transition of these compounds is involved in intramolecular charge transfert between the donor and acceptor fragments. Moreover, we conclude that ICT can be effectively promoted by introducing a Thieno quinoxaline (C8) or Thieno pyredaline (C9) π-lincker acceptors.

3.1.3. Optical properties

3.1.3.1 Absorption properties

For the active materials in organic solar cells, donor compounds play an important role in the

absorption of sunlight because the acceptor PCBM (mostly used in these cells) has a low absorption in the visible and near-infrared region. To examine the optical properties of the studied compounds as donors, a theoretical study based on time-dependent density functional theory (TD-DFT) was used.

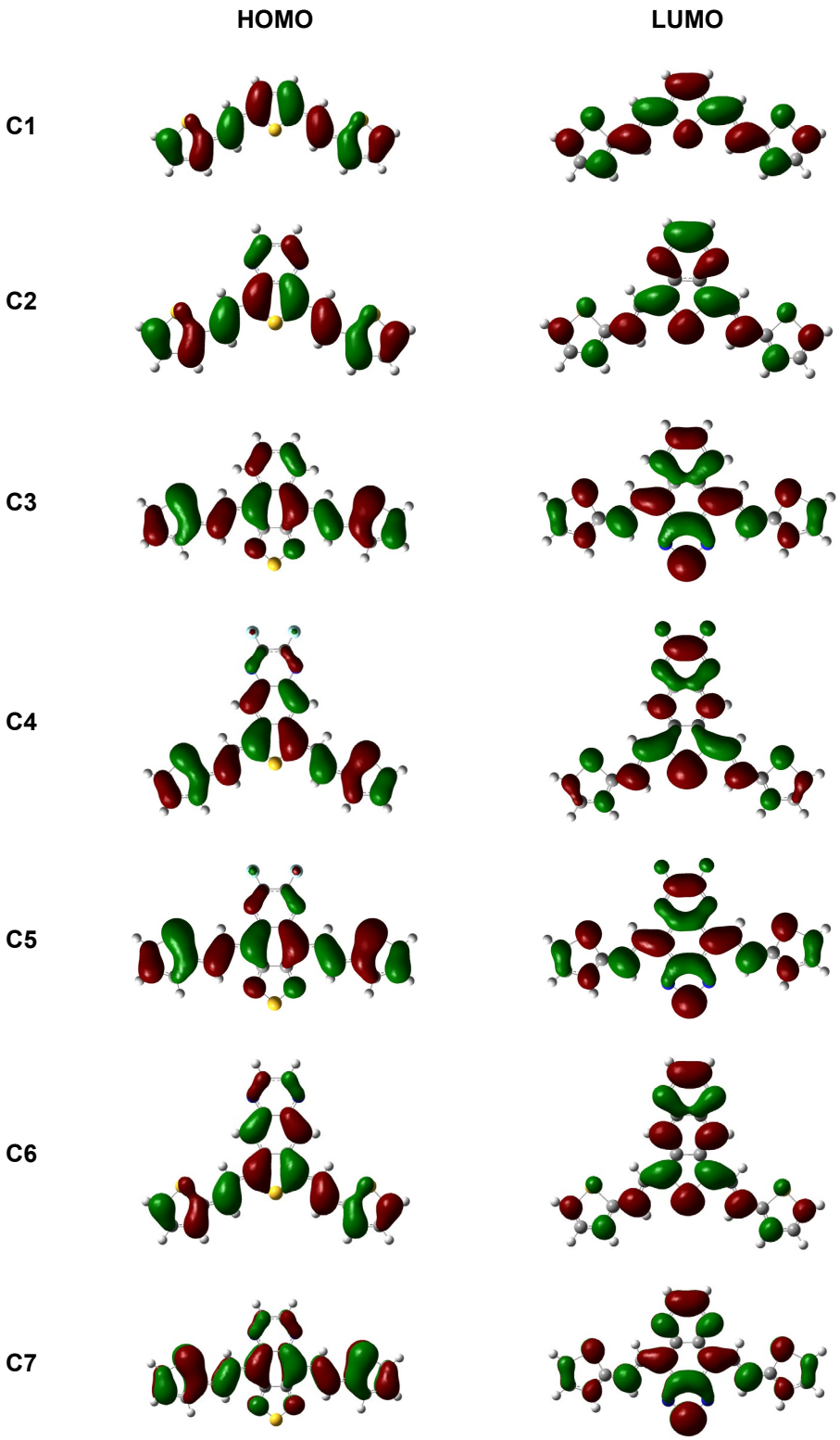

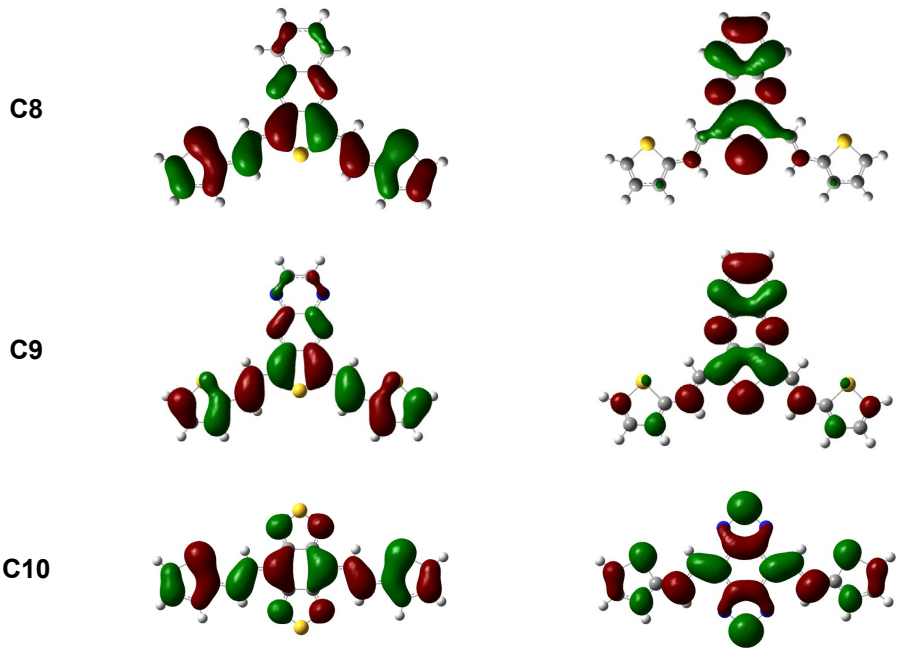

Figure 3. Electronic distribution density of the HOMO and LUMO orbitals of the studied molecules.

Basing on the optimized structures obtained by the B3LYP/6-31G (d, p) method in the ground state, the vertical excitation energies, oscillator strengths for electronic excitations and compositions of vertical transitions in terms of molecular orbital were calculated by using the TD-DFT/CAM-B3LYP/6-31G (d, p) method. The obtained spectroscopic parameters are summarized in Table 3. We noted that all electronic transitions from the ground state (S0) to the first excited state (S1) correspond to HOMO→LUMO transition for all molecules, which can be attributed to the intramolecular charge transfer from donor to acceptor units and π-π* transition. Moreover, the studied molecules absorb mainly the sunlight in visible region, and the maximum absorption wavelength (λ_{max}) of these molecules ranges from 404 to 819 nm. Compared with C1, the maximum absorption is remarkably red shift (bathochromic effect) passing from C2 to C10 in the order C1 < C2 < C3 < C4 < C5 < C6 < C7 < C8 < C9 < C10 which is the excellent agreement of the reverse order of the gap energy. This can be attributed to the increasing of electron-withdrawing strength of the incorporated acceptor units. Consequently, the obtained results suggest these molecules as excellent chromophores and good candidates for organic solar cells applications.

3.1.3.2 Emission properties

To study the photoluminescence emission properties of the compounds, we applied the TDDFT / CAM-B3LYP/6-31(d, p) method to the geometry of the lowest singlet excited state optimized at the CAM-B3LYP / 6-31 (d, p) method. Generally, the emission energy is always lower than the absorption energy, this effect was observed by G. G. Stokes in 1852 [22]. The Stokes displacement (SD) corresponds to the difference between the maximum of absorption λ_{max}^{abs} of the S0→S1 transition and the maximum emission λ_{max}^{em} corresponding to the S1→S0 transition. The calculated emission parameters, S0→S1 transition characters and the Stokes displacements $(\lambda_{max}^{em} - \lambda_{max}^{abs})$ are presented in Table 4.

The obtained results analysis shows that all electronic transitions from the first excited state (S1) to the ground state (S0) correspond to π*-π and LUMO→HOMO transition for all compounds. This shows that the fluorescence phenomenon is the reverse of the absorption process. Moreover, we noted that the emission photoluminescence spectra is red-shifted passing from C10 to C1 which in the reverse order of the obtained results of absorption. Therefore, all compounds haven't high values of stocks shift which ranges from 66 to 225 nm, which reveals that the studied compounds present a maximal conformational

reorganization between ground state and excited state. In addition, this improves the intramolecular charge transfert and the electron injection from LUMO of these molecules to the LUMO of PCBM.

Table 3. Absorption wavelengths (λ_{abs}/nm), vertical transition energies (eV), main transition contribution and oscillator strength (f) of all compounds.

Ci	Transition	λ_{abs} (Exp.)	E_{tr}	f	Transition character in %
C1	S0 → S1	404.16 (424) [21]	3.06	1.40	HOMO → LUMO+1 (95%)
	S0 → S2	291.05	4.25	0.14	HOMO-1 → LUMO (48%)
	S0 → S3	277.92	4.46	0.01	HOMO → LUMO+1 (46%)
	S0 → S4	252.79	4.90	0.06	HOMO-4 → LUMO (85%)
C2	S0 → S1	543.40	2.28	0.77	HOMO → LUMO (97%)
	S0 → S2	351.24	3.52	0.01	HOMO-5 → LUMO (77%)
	S0 → S3	345.52	3.58	0.62	HOMO → LUMO+1 (92%)
	S0 → S4	332.09	3.73	0.11	HOMO-1 → LUMO (92%)
C3	S0 → S1	638.20	1.94	0.60	HOMO → LUMO (98%)
	S0 → S2	369.41	3.35	0.02	HOMO-1 → LUMO (95%)
	S0 → S3	350.41	3.53	0.91	HOMO → LUMO+1 (92%)
	S0 → S4	336.49	3.68	0.10	HOMO-4 → LUMO (94%)
C4	S0 → S1	628.04	1.97	0.58	HOMO → LUMO (98%)
	S0 → S2	397.90	3.11	0.52	HOMO → LUMO+1 (95%)
	S0 → S3	349.09	3.55	0.06	HOMO-1 → LUMO (66%)
	S0 → S4	329.66	3.76	0.45	HOMO → LUMO+2 (59%)
C5	S0 → S1	638.03	1.94	0.64	HOMO → L UMO (98%)
	S0 → S2	391.43	3.16	0.01	HOMO-1 → LUMO (96%)
	S0 → S3	339.55	3.65	1.12	HOMO → LUMO+1 (89%)
	S0 → S4	335.28	3.69	0.01	HOMO → LUMO+2 (95%)
C6	S0 → S1	649.22	1.90	0.56	HOMO → LUMO (99%)
	S0 → S2	403.63	3.07	0.52	HOMO → LUMO+1 (94%)
	S0 → S3	363.23	3.41	0.01	HOMO-4 → LUMO (62%)
	S0 → S4	352.00	3.52	0.03	HOMO-1 → LUMO (58%)
C7	S0 → S1	669.02	1.85	0.61	HOMO → LUMO (98%)
	S0 → S2	395.63	3.13	0.01	HOMO-1 → LUMO (96%)
	S0 → S3	383.67	3.23	0.01	HOMO-5 → LUMO (84%)
	S0 → S4	343.77	3.60	1.08	HOMO → LUMO+1 (85%)
C8	S0 → S1	696.10	1.78	0.27	HOMO → LUMO (97%)
	S0 → S2	393.49	3.15	0.04	HOMO-1 → LUMO (87%)
	S0 → S3	388.43	3.19	0.83	HOMO → LUMO+1 (88%)
	S0 → S4	368.73	3.36	0.01	HOMO-3 → LUMO (97%)
C9	S0 → S1	773.54	1.60	0.33	HOMO → L UMO (98%)
	S0 → S2	473.68	2.61	0.01	HOMO-2 → LUMO (86%)
	S0 → S3	401.95	3.08	0.96	HOMO → LUMO+1 (94%)
	S0 → S4	386.15	3.21	0.17	HOMO-1 → LUMO (90%)
C10	S0 → S1	819.45	1.51	0.52	HOMO → LUMO (100%)
	S0 → S2	420.38	2.94	0.01	HOMO-1 → LUMO (96%)
	S0 → S3	365.72	3.39	0.18	HOMO → LUMO+2 (87%)
	S0 → S4	358.47	3.45	1.01	HOMO → LUMO+1 (83%)

Table 4. The maximum wavelengths emission λ_{max}^{em} (nm), the transition energies E_{tr} (eV), the oscillation strength f and the Stockes shift SS (nm) of the studied compounds.

Ci	Transition	Transition character	λ_{max}^{em} (λ_{Exp})	E_{tr}	f	SS
C1	S1 → S0	LUMO → HOMO (0.69)	470.38 (512) [21]	2.63	1.37	66.22
C2	S1 → S0	LUMO → HOMO (0.69)	654.95	1.89	0.61	111.55
C3	S1 → S0	LUMO → HOMO (0.70)	756.02	1.64	0.50	117.82
C4	S1 → S0	LUMO → HOMO (0.70)	740.55	1.67	0.45	112.51
C5	S1 → S0	LUMO → HOMO (0.70)	763.25	1.62	0.53	125.22
C6	S1 → S0	LUMO → HOMO (0.70)	764.36	1.62	0.44	115.14
C7	S1 → S0	LUMO → HOMO (0.70)	802.42	1.54	0.50	133.40
C8	S1 → S0	LUMO → HOMO (0.70)	849.64	1.45	0.34	153.54
C9	S1 → S0	LUMO → HOMO (0.70)	963.76	1.24	0.23	225.63
C10	S1 → S0	LUMO → HOMO (0.71)	999.17	1.28	0.43	144.31

3.2 Charge transfer properties

3.2.1 Dissociation energy of exciton

It is well known that the binding energy of an exciton (electron-hole) noted E_b, can also be used to give information on the capacity of exciton dissociation. The low E_b value facilitates exciton dissociation. In general, E_b can be expressed using the following relation [23]:

$$E_b = |\Delta H_{H-L} - E_{S1}| \quad (2)$$

ΔE_{H-L} is the difference energy between HOMO and LUMO in the ground state and E_{S1} is the energy of the first excitation (S0→S1).

Table 5. E_{S1} and E_b energy values for Ci molecules (i=1 to 10).

Molecule	C1	C2	C3	C4	C5	C6	C7	C8	C9	C10
E_{S1}	3.06	2.28	1.94	1.97	1.94	1.90	1.85	1.47	1.60	1.51
E_b	0.23	0.17	0.12	0.19	0.18	0.17	0.16	0.18	0.12	0.11

The obtained results of E_b calculations are shown in Table 5, it can be seen that all molecules have low E_b values [24], which are lower than 0.2 eV (with the exception of the C1 molecule of E_b = 0.23 eV), this energy decreases in the following order: C1 > C4 > C5 = C8 > C2 = C6 > C7 > C3 = C9 > C10. This show that these compounds will be able to more effectively promote exciton separation and potentially improve the short-circuit current (Jsc).

3.2.2 Charge transport and reorganization energy

As donor materials, they should have a good charge transport capacity (of electrons and holes), which contributes to the increase of Jsc. The charge transport mechanism can be described as a self-exchange transfer process, in which an electron or hole hops from one charged molecule to an adjacent neutral molecule. The intermolecular charge transfer rate (K_{CT}) can be estimated by Marcus' semi-classical theory according to the following expression [25]:

$$K_{CT} = V^2 \sqrt{\frac{\pi}{\hbar^2 K_B T \lambda}} \exp\left(-\frac{\lambda}{4 K_B T}\right) \quad (3)$$

Here:

V: is the integral of charge transfer (electronic coupling between adjacent molecules),

ħ: is Planck's constant,

K_B: is Boltzmann's constant,

T: the temperature in Kelvin,

λ: is the reorganization energy.

The electronic coupling V and the reorganization energy λ are two key parameters that determine the rate of charge transfer, and they must be maximized and minimized respectively to ensure a high charge transfer rate. In the case of a similar compounds family, the V effect can be neglected in front of λ, this has been shown by studies carried out by Chakanoue's team [26].

In general, the reorganization energy is composed of both the intramolecular reorganization energy of the molecule (inner λ) and the reorganization energy of the surrounding medium (outer λ) [27,28]. In this work, the external λ is induced by the slow electronic and nuclear variations in solvent polarization of the surrounding medium is neglected [29]. Consequently, the internal contribution becomes the dominant factor. In this study, we calculated the reorganization energy of holes and electrons (λ^+ and λ^-) by a potential energy surface curve method according to the following expression [30]:

$$\lambda^{\pm} = [E^{\pm}(M^0) - E^{\pm}(M^{\pm})] + [E^0(M^{\pm}) - E^0(M^0)] \quad (4)$$

Here:

$E^0(M^0)$: is the total energy of the neutral molecule,

$E^{\pm}(M^0)$: is the total energy of the cationic (anionic) form with neutral form geometry,

$E^{\pm}(M^{\pm})$: is the total energy of the cationic (anionic) form,

$E^0(M^{\pm})$: is the total energy of the neutral form with cation (anion) geometry.

The calculated values of λ^+, λ^- and the total

reorganization energy λ (= $\lambda^+ + \lambda^-$) of all molecules are shown in Table 7.

Table 6. Reorganization energies of Ci molecules (i = 1 to 10) in eV.

Molecule	C1	C2	C3	C4	C5	C6	C7	C8	C9	C10
λ^+	0.25	0.27	0.27	0.28	0.30	0.27	0.29	0.27	0.29	0.30
λ^-	0.25	0.27	0.27	0.28	0.30	0.27	0.29	0.27	0.29	0.30
λ	0.50	0.54	0.54	0.56	0.60	0.54	0.58	0.54	0.58	0.60

From the obtained results of the Table 6, we observed that the λ^+ and λ^- values are identical for each molecule, this indicate an excellent balanced transport of both electrons and holes. As mentioned previously, the weak λ value increases the K_{CT}. Moreover, we note that all Ci show small λ^+, λ^- and λ values which range from 0.27 to 0.30 eV (λ^+ and λ^-) and from 0.54 to 0.60 eV (λ). This improves the ICT and suggests these molecules as well charge transport materials for organic solar cells.

3.3. Photovoltaic performance of the studied systems in a BHJ cell

3.3.1 Photovoltaic parameters

In organic solar cells especially in bulk heterojunction (BHJ) active layer, the analysis of frontier orbitals energies of the molecular orbital frontiers (HOMO and LUMO) of the studied compounds as donors and compared with the LUMO energy level of the fullerene derivative acceptors (Figure 4) which is the most broadly used as an acceptor in solar cell devices. These parameters are very important factors to determine whether effective charge transfer will happen from HOMO of donor (studied molecules) to LUMO of acceptor (PCBM). Moreover, the maximum open circuit voltage (Voc) of the bulk hetero junction (BHJ) solar cell is related to the energy difference between HOMO of donor and LUMO of the acceptor, taking into account the energy lost during the photo-charge generation [31]. The estimated values of Voc have been calculated from the following formula:

$$Voc = |E_{HOMO}\ (Donor)| - |E_{LUMO}\ (Acceptor)| - 0.3 \quad (5)$$

Another photovoltaic parameter noted α which was calculated as the energy difference between LUMO of donor and LUMO of the acceptor. This parameter must be greater than 0.3 eV but not too high (between 0.3 and 0.5 eV) to ensure efficient dissociation of excitons at the D/A interface [32, 33].

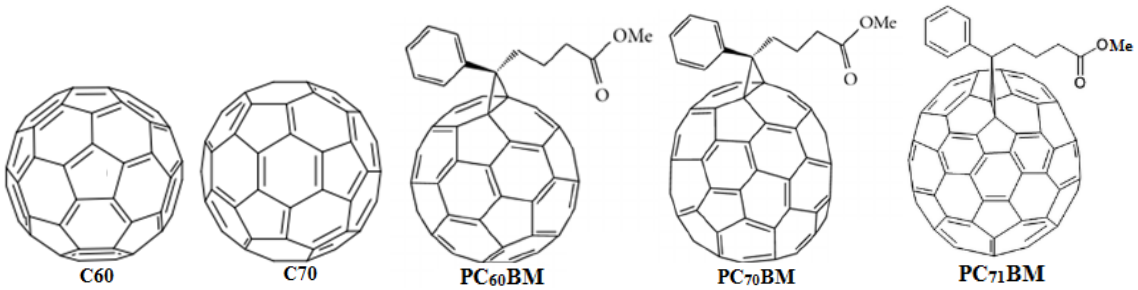

Figure 4. C60, C70, $PC_{70}BM$, $PC_{60}BM$ and $PC_{71}BM$ acceptor structures.

Table 7 summarized data of energy frontier orbitals of all compounds and of acceptors: $PC_{70}BM$, $PC_{60}BM$ and $PC_{71}BM$, Voc and α. We notice that energy HOMO of all compounds is higher than LUMO of the acceptors and the Voc calculate values of the studied compounds (donor) blended with PCBM ($PC_{70}BM$, $PC_{60}BM$ or $PC_{71}BM$) in the active layer of BHJ range from 0.65 to 1.21V with $PC_{70}BM$, from 0.59 to 1.05V with $PC_{60}BM$ and from 0.35 to 0.81V with $PC_{71}BM$. These values are sufficient for an efficient electron injection from the Ci molecules (donors) to the PCBM acceptors. In addition, α range from -0.13 to 1.48 eV with $PC_{70}BM$, 0.27 to 1.64 eV with $PC_{60}BM$ and 0.51 to 1.88 eV with $PC_{71}BM$, this shows that the dissociation of the excitons at the

D/A interface will take place except for C10 in coupling with $PC_{70}BM$ the value from α is negative, this reveals that the electron injection will be impossible from C10 to $PC_{70}BM$.

Table 7. Calculated values of Voc (in V) and α in (eV) for the systems studied in relation to PCBM and PCBM A acceptors.

Molecule	E_{HOMO} (eV)	E_{LUMO} (eV)	Voc			α		
			$PC_{70}BM$	$PC_{60}BM$	$PC_{71}BM$	$PC_{70}BM$	$PC_{60}BM$	$PC_{71}BM$
C1	-4.89	-2.06	1.05	0.89	0.65	1.48	1.64	1.88
C2	-4.80	-2.69	0.96	0.80	0.56	0.85	1.01	1.25
C3	-4.76	-2.94	0.92	0.76	0.52	0.60	0.76	1.00
C4	-4.73	-2.95	0.89	0.73	0.49	0.59	0.75	0.99
C5	-5.05	-3.29	1.21	1.05	0.81	0.25	0.41	0.65
C6	-4.59	-2.85	0.65	0.59	0.35	0.69	0.85	1.09
C7	-4.88	-3.19	1.04	0.88	0.64	0.35	0.51	0.75
C8	-4.63	-2.98	0.79	0.63	0.39	0.56	0.72	0.96
C9	-4.82	-3.34	0.98	0.82	0.58	0.20	0.36	0.60
C10	-4.83	-3.43	0.99	0.83	0.59	- 0.13	0.27	0.51
$PC_{70}BM$ **[34]**	- 5.87	-3.54						
$PC_{60}BM$ **[35]**	-6.10	-3.70						
$PC_{71}BM$ **[36]**	-5.93	-3.94						

3.3.2 Conversion efficiency

We have estimated the conversion efficiency of maximum power of the studied molecules in a BHJ photovoltaic cell with ITO/Ci:PCBM/Al architecture by using Scharber's model [37].

According to Figure 5 and Table 8 data, the conversion efficiency of the photovoltaic cells ranges from 5 to ≥10%/$PC_{70}BM$, from 4 to 10%/$PC_{60}BM$ and from 2 to 8%/$PC_{71}BM$. The higher conversion efficiencies is 10% with C9: $PC_{70}BM$ and C7: $PC_{60}BM$ couples.

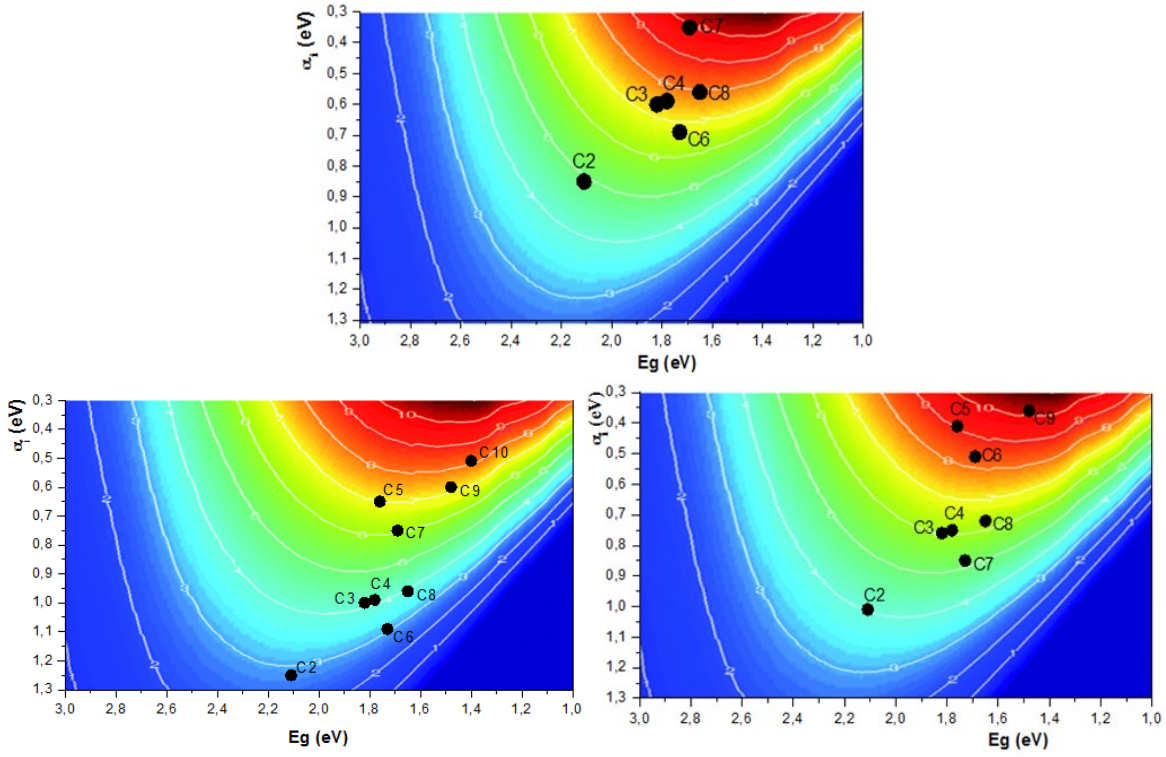

Figure 5. Estimation of the photovoltaic conversion efficiency of the compounds studied with $PC_{70}BM$ (top right), $PC_{60}BM$ (top left) and $PC_{71}BM$ (bottom) according to Scharber's model.

Table 8. Estimated conversion efficiencies according to Scharber's model for the different Ci:PCBM couples.

Compound	Conversion efficiency in %		
	$PC_{70}BM$	$PC_{60}BM$	$PC_{71}BM$
C2	5	4	2
C3	7	6	4
C4	7	6	4
C5	-	9	7
C6	6	8	3
C7	**10**	5	6
C8	8	6	4
C9	-	**10**	7
C10	-	-	8

4. Conclusions

In this work, ten D-A-D type small molecules based on Thienylenevinylene and different heterocyclic acceptors as bridges were theoretically studied using DFT/B3LYP/6-31G(d,p) and TDDFT/CAM-B3LYP/6-31G(d,p) methods, in order to investigate the geometric, the optoelectronic and photovoltaic properties, also to determine the effect of acceptor bridge on these properties, then to improve the conversion efficiency of the studied compounds for organic solar cells application. The geometrical analysis of the optimized structures of these materials shows that all compounds have planar structures. Comparing with C1, the introduction of heterocyclic acceptors as bridge reduces the gap energies from 2.82 to 1.40 eV in the following order: C1 < C2 < C3 < C4 < C5 < C6 < C7 < C8 < C9 < C10. All molecules absorb in the visible region and their absorption wavelengths range from 404 to 819 nm with a bathochromic shift passing from C1 to C10, indicating that spectra of these compounds cover well the spectra emitted from sunlight. Moreover, the calculated values of E_b and λ indicate higher exciton dissociation efficiency and well charge transfer. In addition, the Voc and α of the studied molecules blended with different acceptors ($PC_{60}BM$, $PC_{70}BM$ and $PC_{71}BM$) range from 0.70 to 0.94 eV and from 0.2 to 1.8 eV respectively, indicating that these values are sufficient for an efficient electron injection from Ci to PCBM. Finally, the photovoltaic cells which contain these materials (donors) coupled with several acceptors (PCBM) present high conversion efficiency which can reaches 10% for the couples C7: $PC_{70}BM$ and C9: $PC_{60}BM$. At the same time, it is important to note that these results do not exclude the potential of these studied compounds in applications in other optoelectronic devices.

References and Notes

[1] Sharma, G. D.; Mikroyannidis, J. A.; Sharma, S. S.; Thomas, K. R. J. *Dyes Pigm.* **2012**, *94*, 320. [Crossref]

[2] Lin, Y.; Cheng, P.; Liu, Y.; Shi, Q.; Hu, W.; Li, Y.; Zhan, X. *Org. Electron.* **2012**, *13*, 673. [Crossref]

[3] Lin, H. W.; Kang, H. W.; Huang, Z. Y.; Chen, C. W.; Chen, Y. H.; Lin, L. Y.; Lin, F.; Wong, K. T. *Org. Electron.* **2012**, *13*, 1925. [Crossref]

[4] Lin, H. W.; Chen, Y. H.; Huang, Z. Y.; Chen, C. W.; Lin, L. Y.; Lin, F.; Wong, K. T. *Org. Electron.* **2012**, *13*, 1722. [Crossref]

[5] Fitzner, R.; Elschner, C.; Weil, M.; Uhrich, C.; Korner, C.; Riede, M.; Leo, K.; Pfeiffer, M.; Reinold, E.; Osteritz, E. M.; Bauerle, P. *Adv. Mater.* **2012**, *24*, 675. [Crossref]

[6] Chen, Y. H.; Lin, L. Y.; Lu, C. W.; Lin, F.; Huang, Z. Y.; Lin, H. W.; Wang, P. H.; Liu, Y. H.; Wong, K. T.; Wen, J.; Miller, D. J.; Darling, S. B. *J. Am. Chem. Soc.* **2012**, *134*, 13616. [Crossref]

[7] Steinberger, S.; Mishra, A.; Reinold, E.; Levichkov, J.; Uhrich, C.; Pfeiffer, M.; Bauerle, P. *Chem. Commun.* **2011**, *47*, 1982. [Crossref]

[8] Liu, Y.; Wan, X.; Wang, F.; Zhou, J.; Long, G.; Tian, J.; You, J.; Yang, Y.; Chen, Y. *Adv. Energy Mater.* **2011**, *1*, 771. [Crossref]

[9] Lin, L. Y.; Chen, Y. H.; Huang, Z. Y.; Lin, H. W.; Chou, S. H.; Lin, F.; Chen, C. W.; Liu, Y. H.; Wong, K. T. J. *Am. Chem. Soc.* **2011**, *133*, 15822. [Crossref]

[10] Chen, Y. H.; Lin, L. Y.; Lu, C. W.; Lin, F.; Huang, Z. Y.; Lin, H. W.; Wang, P. H.; Liu, Y. H.; Wong, J.; Wen, K. T.; Miller, D. J.; Darling, S. B. *J. Am. Chem. Soc.* **2012**, *134*, 13616. [Crossref]

[11] Rousseau, T.; Cravino, A.; Bura, T.; Ulrich, G.; Ziessel, R.; Roncali, J. *J. Mater. Chem.* **2009**, *19*, 2298. [Crossref]

[12] Frisch, M.; Trucks, G. W.; Schlegel, H. B.; Scuseria, G. E.; Robb, M. A.; Cheeseman, J. R.; Scalmani, G.; Barone, V.; Mennucci, B.; Petersson, G. A.; Others, Gaussian 09, Revision D. 2009,01.

[13] Becke, A. D. J. *Chem. Phys.* **1993**, *98*, 5648. [Crossref]

[14] Mikroyannidis, J. A.; Tsagkournos, D. V.; Balraju, P.; Sharma, G. D. *J. Power Sources* **2011**, *196*, 4152. [Crossref]

[15] Yanai, T.; Tew, D. P.; Handy, N. C. *Chem. Phys. Lett.* **2004**, *393*, 51. [Crossref]

[16] Yang, Z.; Liu, C.; Shao, C.; Lin, C.; Liu, Y. *J. Phys. Chem.* **2015**, *119*, 21852. [Crossref]

[17] Katono, K.; Bessho, T.; Wielopolski, M.; Marszalek, M.; Moser, J. E.; Humphry-Baker, R.; Zakeeruddin, S. M.; Graatzel, M. *J. Phys. Chem.* **2012**, *116*, 16876. [Crossref]

[18] Rostov, I. V.; Amos, R. D.; Kobayashi, R.; Scalmani, G.; Frisch, M. J. *J. Phys. Chem.* **2010**, *114*, 5547. [Crossref]

[19] Pedone, A. *J. Chem. Theory Comput.* **2013**, *9*, 4087. [Crossref]

[20] Zhang, Z.; Qin, Y. *Macromolecules* **2016**, *49*, 3318. [Crossref]

[21] Tanaka, S.; Fukui, Y.; Koumura, N.; Nakagawa, N.; Mori, A. *Org. Lett.* **2016**, *18*, 650. https://doi.org/10.1021/acs.orglett.5b03567

[22] Stokes, G. G. *Phil. Trans. R. Soc.* **1952**, *142*, 463.

[23] Kose, M. E. *J. Phys. Chem.* **2012**, *116*, 12503. [Crossref]

[24] Clarke, T. M.; Durrant, J. R. *Chem. Rev.* **2010**, *110*, 6736. [Crossref]

[25] Barbara, P. F.; Meyer, T. J.; Ratner, M. A. *J. Phys. Chem.* **1996**, *100*, 13148. [Crossref]

[26] SKanoue, K.; Motoda, M.; Sugimoto, M.; Sakaki, S. *J. Phys. Chem.* **1999**, *103*, 5551. [Crossref]

[27] Sliders, P.; Marcus, R. A. *J. Am. Chem. Soc.* **1981**, *103*, 748. [Crossref]

[28] Brunschwig, B. S.; Logan, J.; Newton, M. D.; Sutin, N. *J. Am. Chem. Soc.* **1980**, *102*, 5798. [Crossref]

[29] Hutchison, G. R.; Ratner, M. A.; Marks, T. J. *J. Am. Chem. Soc.* **2005**, *127*, 2339. [Crossref]

[30] Kose, M. E.; Mitchell, W. J.; Kopidakis, N.; Chang, C. H.; Shaheen, S. E.; Kim, K.; Rumbles, G. *J. Am. Chem. Soc.* **2007**, *129*, 14257. [Crossref]

[31] (a) Zhao, G. J.; He, Y. J.; Li, Y. F. *Adv Mater.* **2010**, *22*, 4355. [Crossref] (b) Baffreau, J.; Lhez, S. L.; Van Anh, N.; Williams, R. M.; Hudhomme, P. *Chem-Eur J.* **2008**, *14*, 4974. [Crossref]

[32] Gadisa, A.; Svensson, M.; Andersson, M. R.; Inganas, O. *Appl. Phys. Lett.* **2004**, *84*, 1609. [Crossref]

[33] (a) Dang, M. T.; Hirsch, L.; Wantz, G. *Adv Mater.* **2011**, *23*, 3597. [Crossref] (b) Dang, M. T.; Hirsch, L.; Wantz, G.; Wuest, J. D. *Chem Rev.* **2013**, *113*, 3734. [Crossref]

[34] He, Y.; Chen, H. Y.; Hou, J.; Li, Y. *J. Am. Chem. Soc.* **2010**, *132*, 1377. [Crossref]

[35] Morvillo, P. *Sol. Energy Mater. Sol. Cells* **2009**, *93*, 1827. [Crossref]

[36] Oh, S.; Badgujar, S.; Kim, D. H.; Lee, W. E.; Khan, N.; Jahandar, M.; Rasool, S.; Song, C. E.; Lee, H. K.; Shin, W. S.; Lee, J. C.; Moon, S. J.; Lee, S. K. *J. Mater. Chem. A* **2017**, *5*, 15923. [Crossref]

[37] Scharber, M. C.; Sariciftci, N. S. *Prog. Polym. Sci.* **2013**, *38*, 1929. [Crossref]